RESEARCH ARTICLE SUMMARY

IMMUNOGENETICS

Epigenetic programming of monocyte-to-macrophage differentiation and trained innate immunity

Sadia Saeed,* Jessica Quintin,* Hindrik H. D. Kerstens,* Nagesha A. Rao,* Ali Aghajanirefah,* Filomena Matarese, Shih-Chin Cheng, Jacqueline Ratter, Kim Berentsen, Martijn A. van der Ent, Nilofar Sharifi, Eva M. Janssen-Megens, Menno Ter Huurne, Amit Mandoli, Tom van Schaik, Aylwin Ng, Frances Burden, Kate Downes, Mattia Frontini, Vinod Kumar, Evangelos J. Giamarellos-Bourboulis, Willem H. Ouwehand, Jos W. M. van der Meer, Leo A. B. Joosten, Cisca Wijmenga, Joost H. A. Martens, Ramnik J. Xavier, Colin Logie,† Mihai G. Netea,† Hendrik G. Stunnenberg†

INTRODUCTION: Monocytes circulate in the bloodstream for up to 3 to 5 days. Concomitantly, immunological imprinting of either tolerance (immunosuppression) or trained immunity (innate immune memory) determines the functional fate of monocytes and monocyte-derived macrophages, as observed after infection or vaccination.

METHODS: Purified circulating monocytes from healthy volunteers were differentiated under the homeostatic macrophage colony-stimulating factor concentrations present in human serum. During the first 24 hours, trained immunity was induced by β-glucan (BG) priming, and postsepsis immunoparalysis was mimicked by exposure to lipopolysaccharide (LPS), generating endotoxin-induced tolerance. Epigenomic profiling of the histone marks H3K4me1, H3K4me3, and H3K27ac, DNase I accessibility, and RNA sequencing were performed at both the start of the experiment (ex vivo monocytes) and at the end of the 6 days of in vitro culture (macrophages).

RESULTS: Compared with monocytes (Mo), naïve macrophages (Mf) display a remodeled metabolic enzyme repertoire and attenuated innate inflammatory pathways, most likely necessary to generate functional tissue macrophages. Epigenetic profiling uncovered about 8000 dynamic regions associated with about 11,000 DNase I hypersensitive sites. Changes in histone acetylation identified most dynamic events. Furthermore, these regions of differential histone marks displayed some degree of DNase I accessibility that was already present in monocytes. H3K4me1 mark increased in parallel with de novo H3K27ac deposition at distal regulatory regions; H3K4me1 mark remained even after the loss of H3K27ac, marking decommissioned regulatory elements.

β-glucan priming specifically induced about 3000 distal regulatory elements, whereas LPS tolerization induced H3K27ac at about 500 distal regulatory regions. At the transcriptional level, we identified co-regulated gene modules during monocyte-to-macrophage differentiation, as well as discordant modules between trained and tolerized cells. These indicate that training likely involves an increased expression of modules expressed in naïve macrophages, including genes that code for metabolic enzymes. On the other hand, endotoxin tolerance involves gene modules that are more active in monocytes than in naïve macrophages. About 12% of known human transcription factors display variation in expression during macrophage differentiation, training, and tolerance. We also observed transcription factor motifs in DNase I hypersensitive sites at condition-specific dynamic epigenomic regions, implying that specific transcription factors are required for trained and tolerized macrophage epigenetic and transcriptional programs. Finally, our analyses and functional validation indicate that the inhibition of cyclic adenosine monophosphate generation blocked trained immunity in vitro and during an in vivo model of lethal *Candida albicans* infection, abolishing the protective effects of trained immunity.

ON OUR WEB SITE

Read the full article at http://dx.doi.org/10.1126/science.1251086

DISCUSSION: We documented the importance of epigenetic regulation of the immunological pathways underlying monocyte-to-macrophage differentiation and trained immunity. These dynamic epigenetic elements may inform on potential pharmacological targets that modulate innate immunity. Altogether, we uncovered the epigenetic and transcriptional programs of monocyte differentiation to macrophages that distinguish tolerant and trained macrophage phenotypes, providing a resource to further understand and manipulate immune-mediated responses. ■

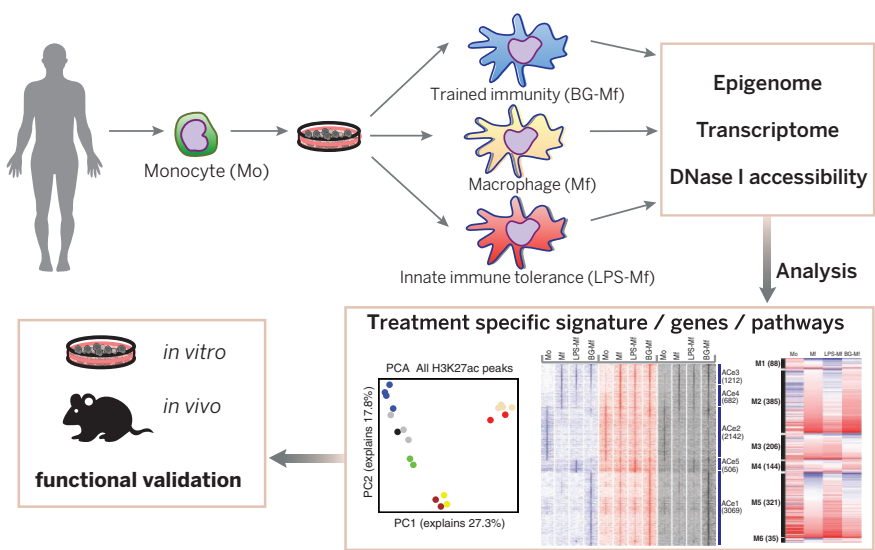

The epigenome, DNase I accessibility, and transcriptome were characterized in purified human circulating monocytes, in vitro differentiated naïve, tolerized (immunosuppression), and trained macrophages (innate immune memory). This allowed the identification of pathways functionally implicated in innate immune memory. This epigenetic signature of human monocyte-to-macrophage differentiation and monocyte training generates hypotheses to understand and manipulate medically relevant immune conditions.

The list of author affiliations is available in the full article online.
*These authors contributed equally to this work.
†Corresponding author. E-mail: h.stunnenberg@ncmls.ru.nl (H.G.S.); mihai.netea@radboudumc.nl (M.G.N.); c.logie@ncmls.ru.nl (C.L.)
Cite this article as S. Saeed *et al.*, *Science* **345**, 1251086 (2014); DOI: 10.1126/science.1251086

RESEARCH ARTICLE

IMMUNOGENETICS

Epigenetic programming of monocyte-to-macrophage differentiation and trained innate immunity

Sadia Saeed,[1]* Jessica Quintin,[2]* Hindrik H. D. Kerstens,[1]* Nagesha A. Rao,[1]* Ali Aghajanirefah,[1]* Filomena Matarese,[1] Shih-Chin Cheng,[2] Jacqueline Ratter,[2] Kim Berentsen,[1] Martijn A. van der Ent,[1] Nilofar Sharifi,[1] Eva M. Janssen-Megens,[1] Menno Ter Huurne,[1] Amit Mandoli,[1] Tom van Schaik,[1] Aylwin Ng,[3,4] Frances Burden,[5,6] Kate Downes,[5,6] Mattia Frontini,[5,6] Vinod Kumar,[7] Evangelos J. Giamarellos-Bourboulis,[8] Willem H. Ouwehand,[5,6] Jos W. M. van der Meer,[2] Leo A. B. Joosten,[2] Cisca Wijmenga,[7] Joost H. A. Martens,[1] Ramnik J. Xavier,[3,4] Colin Logie,[1]† Mihai G. Netea,[2]† Hendrik G. Stunnenberg[1]†

Monocyte differentiation into macrophages represents a cornerstone process for host defense. Concomitantly, immunological imprinting of either tolerance or trained immunity determines the functional fate of macrophages and susceptibility to secondary infections. We characterized the transcriptomes and epigenomes in four primary cell types: monocytes and in vitro–differentiated naïve, tolerized, and trained macrophages. Inflammatory and metabolic pathways were modulated in macrophages, including decreased inflammasome activation, and we identified pathways functionally implicated in trained immunity. β-glucan training elicits an exclusive epigenetic signature, revealing a complex network of enhancers and promoters. Analysis of transcription factor motifs in deoxyribonuclease I hypersensitive sites at cell-type–specific epigenetic loci unveiled differentiation and treatment-specific repertoires. Altogether, we provide a resource to understand the epigenetic changes that underlie innate immunity in humans.

Monocytes are generally considered as an intermediate developmental stage between bone marrow precursors and tissue macrophages (*1*). However, circulating monocytes have important effector functions, both during homeostasis through patrol and repair functions (*2*) and during infections by exerting inflammatory effects (*3*). Although several populations of tissue-resident macrophages originate from yolk sac embryonic precursors (*4*), tissues such as dermis and the intestine contain adult monocyte-derived macrophages (*5*–*7*), whereas during infections, adult blood inflammatory monocytes migrate to inflamed tissues and differentiate into monocyte-derived macrophage populations that can eliminate the pathogen and restore tissue integrity (*8*).

In homeostasis or during infections, monocytes can follow different functional programs. During the process of tolerance/immunoparalysis, a common complication of severe sepsis, monocytes enter a refractory functional state, characterized by the incapacity to produce proinflammatory cytokines and decreased human leukocyte antigen DR expression (*9*). Tolerance can be mimicked in vitro and in vivo by challenging the cells with endotoxins such as lipopolysaccharide (LPS): After an initial stimulation phase, cells enter a state of long-term immunotolerance. In contrast, other infections or vaccinations [e.g., *Candida albicans* infection, Bacille Calmette-Guerin (BCG), or measles vaccination] increase the long-term responsiveness of monocytes to microbial stimuli, a state termed "trained immunity" that confers resistance to secondary infections (*10*–*14*). In the case of *Candida* infection, training requires the β-glucan receptor Dectin-1 and the noncanonical Raf-1 pathway and is associated with stable changes in histone trimethylation at H3K4 at a small subset of promoters (*10*). Tolerance and training represent clinically relevant functional states such as the immune paralysis encountered during bacterial sepsis or endotoxin shock (*9*) or the nonspecific protective effects of live microorganism vaccination [e.g., BCG, measles, and yellow fever (*15*)] and strongly influence susceptibility to secondary infections.

Histone and DNA modifications have been hypothesized to play a role in regulating monocyte and macrophage phenotypes (*16*), but data are limited to a few genes and histone modifications (*17*). Moreover, the epigenetic modifications after LPS stimulation were studied for relatively short periods of up to 1 day (*18*). In addition, the two major events that determine the functional fate of monocytes and macrophages—immune tolerance (*19*) and innate immune training (*10*)—have not been thoroughly characterized at the transcriptional and epigenomic level. The BLUEPRINT Consortium aims at defining the epigenomic maps and transcription profiles of a wide variety of blood cells from healthy primary human cells as well as blood-based diseases (*20*, *21*) (www.blueprint-epigenome.eu). Here, we report on the epigenome and transcriptome of monocyte-to-macrophage differentiation and the response to tolerance and training.

Monocyte differentiation in response to external stimuli

Upon migration into the tissues, monocytes differentiate into tissue macrophages. In addition, under differential inflammatory conditions, monocytes can be directed into tolerance or trained immunity functional programs (Fig. 1A). To analyze the different functional programs of monocytes and macrophages, human circulating monocytes (Mo) were purified by triple depletion of T and B lymphocytes and natural killer (NK) cells from the peripheral blood mononuclear cells of healthy human volunteers (fig. S1). Fluorescence-activated cell sorting and transcriptome analyses revealed high-purity monocytes similar to cell surface markers of $CD14^+$ positively selected monocytes (fig. S1).

Using an in vitro approach, we differentiated Mo into macrophages (Mf) by long-term incubation in medium supplemented with human serum (*22*). Alternatively, monocytes were exposed for the first 24 hours to LPS to induce endotoxin tolerance (immune paralysis) (Fig. 1, A and B) (*9*). The LPS exposure of monocytes induced long-term tolerant cells (LPS-Mf) that produce less proinflammatory mediators, such as tumor necrosis factor–α (TNF-α) and interleukin-6 (IL-6), upon an immune challenge with tripalmitoyl glyceryl cysteine (Pam3Cys, a ligand of TLR2) than unprimed naïve Mf. In contrast, a short priming of monocytes with β-glucan induces trained immune cells (BG-Mf) (Fig. 1, A and B) (*10*) that are characterized by an enhanced inflammatory status (*10*) (Fig. 1B). On the basis of the expression of cell surface markers, we concluded that LPS and β-glucan priming followed by continued culture for 5 days yields macrophage-like cells, but with distinct functional programs

[1]Department of Molecular Biology, Faculties of Science and Medicine, Radboud Institute for Molecular Life Sciences, Radboud University, 6500 HB Nijmegen, Netherlands. [2]Department of Internal Medicine, Radboud University Medical Center, 6525 GA Nijmegen, Netherlands. [3]Center for Computational and Integrative Biology and Gastrointestinal Unit, Massachusetts General Hospital, Harvard School of Medicine, Boston, MA 02114, USA. [4]Broad Institute of Massachusetts Institute of Technology and Harvard University, Cambridge, MA 02142, USA. [5]Department of Haematology, University of Cambridge, Cambridge, UK. [6]National Health Service, Blood and Transplant Cambridge Centre, Cambridge Biomedical Campus, Cambridge CB0 2PT, UK. [7]University of Groningen, University Medical Center Groningen, Department of Genetics, Groningen, Netherlands. [8]Fourth Department of Internal Medicine, University of Athens, Medical School, 1 Rimini Street, 12462 Athens, Greece.
*These authors contributed equally to this work. †**Corresponding authors. E-mail: h.stunnenberg@ncmls.ru.nl (H.G.S.); mihai.netea@radboudumc.nl (M.G.N.); c.logie@ncmls.ru.nl (C.L.)**

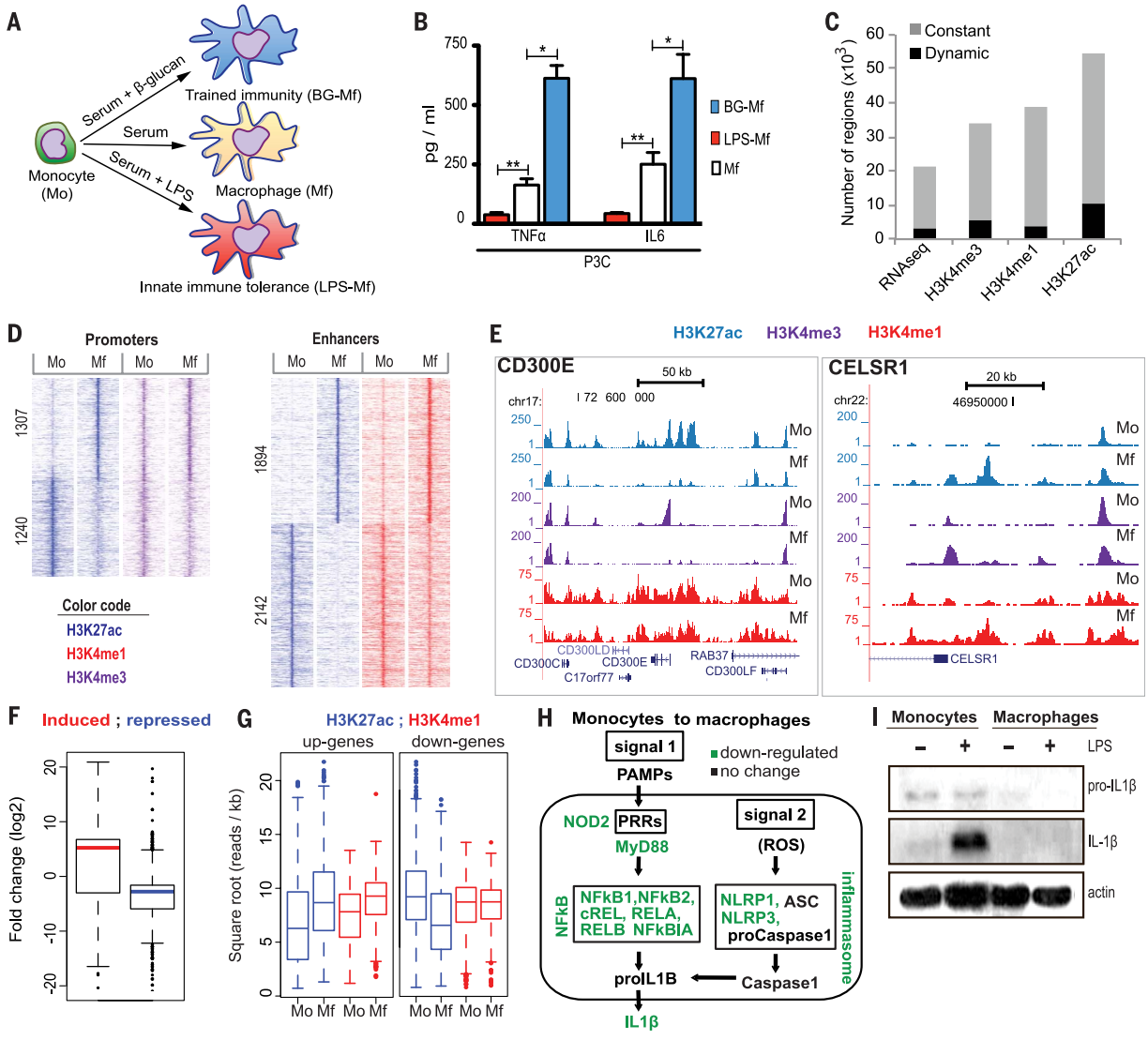

J Genes repressed upon differentiation

GO term	Pvalue	Bonferroni
response to wounding	1.30E-16	9.00E-14
inflammatory response	1.10E-15	6.00E-13
cytokine activity	3.80E-09	3.30E-06
extracellular region part	1.50E-06	3.30E-04
chemokine receptor binding	5.60E-05	4.80E-03

Genes induced upon differentiation

GO term	Pvalue	Bonferroni
cytoplasmic part	1.70E-29	8.20E-27
mitochondrion	4.80E-27	1.20E-24
cellular ketone metabolic process	1.10E-20	3.40E-17
carboxylic acid metabolic process	2.70E-20	8.40E-17
organic acid metabolic process	4.60E-20	1.40E-16

Fig. 1. Epigenomic and transcriptional changes during monocyte-to-macrophage differentiation. (**A**) Upon migration into tissues under homeostatic conditions, Mo differentiate into Mf. In addition, monocytes will enter into either a refractory state described as endotoxin "tolerance" that is mimicked in vitro with a short LPS stimulation (LPS-Mf) or a state of increased responsiveness described as trained immunity that is mimicked in vitro with a short ß-glucan incubation (BG-Mf) (see also fig. S4E). (**B**) Cytokine production determined by enzyme-linked immunosorbent assay (ELISA) in supernatants of monocytes primed for 24 hours with cell culture medium (Mf), β-glucan (BG-Mf), or LPS (LPS-Mf) and restimulated on day 6 for an additional 24 hours. $*P < 0.05$ and $**P < 0.005$ (Wilcoxon signed-rank test). Data are presented as mean ± SEM (pooled data from $n \geq 10$ individuals in four independent experiments). (**C**) The proportion of dynamic transcripts and epigenetic regions that differ by at least two median absolute deviations for the H3K27ac, H3K4me3, and H3K4me1 epigenetic marks as a function of monocyte differentiation and/or priming regimens. (**D**) Pile-up heat map of the epigenetic marks from (C) at promoters and enhancers in Mo and Mf. Rows are genomic regions from –12 to +12 kb around the center of the peaks; the signal intensity was determined in windows of 400 bp. (**E**) Screen shots of the epigenetic landscape at the CELSR1 (right) or CD300E (left) loci, two representative examples of loci that display important changes during macrophage differentiation. (**F**) Box-plot presentation of changes in transcript levels during differentiation (Mo to Mf) for the closest differentially expressed genes (within 100 kb) from the dynamic H3K27ac marked regions. (**G**) Box-plot presentation of changes in the H3K27ac and H3K4me1 signal at distal H3K27ac binding sites, in the vicinity (closest within 100 kb) of up-regulated (left) and down-regulated (right) genes during Mo-to-Mf differentiation. (**H**) Modulation of the inflammasome and NF-κB pathways during monocyte-to-macrophage differentiation. (**I**) Mo and Mf were left unstimulated (–) or stimulated with LPS (10 ng/mL) for 24 hours (+). Inflammasome activation was determined by Western blot for IL-1β and pro-interleukin-1β (proIL-1β). The results are representative of at least three independent experiments. (**J**) GO analysis. Enriched GO categories in a set of significantly (4-fold change, RPKM > 2) down- and up-regulated genes when comparing Mo to Mf.

(fig. S1). This was supported by our epigenomic and transcriptomic analyses (fig. S3, see below).

Epigenomic profiles were generated for Mo, naïve Mf, LPS-Mf, and BG-Mf (Fig. 1C) for three histone marks positively associated with gene expression: H3K4me3, which marks promoters; H3K4me1, which marks distal regulatory elements (enhancers); and H3K27ac, which marks active promoters and enhancers (*23*, *24*), following the guidelines of the International Human Epigenome Consortium (www.ihec-epigenomes.org). We also examined the DNA accessibility through deoxyribonuclease I sequencing (DNaseI-seq) and RNA-seq (*25*). In total, 17% of the H3K4me3 peaks, 10% of the H3K4me1 blocks, and 19% of the H3K27ac peaks are dynamic, changing during differentiation (Mo relative to Mf, LPS-Mf, and BG-Mf) by at least two median absolute deviations (Fig. 1C). H3K27ac was by far the most dynamic mark, more often fluctuating distally (7611) [termed acetylated elements (ACe)] compared with the regions within 2.5 kb of an annotated transcription start site (TSS), 3063, [termed acetylated promoters (ACp)]. Importantly, all regions examined displayed some degree of DNase I cleavage sensitivity, indicating that the vast majority of locations, including those with the de novo deposition of H3K27ac, are likely accessible to some extent in monocytes before stimulation. (see also Fig. 2).

Epigenetic and transcriptional changes during monocyte-to-macrophage differentiation

Epigenetic alterations during differentiation of Mo into naïve Mf were considered separately at promoters and distal regulatory elements (Fig. 1D). Promoters were operationally defined as regions within 2.5 kb of a TSS that also bear a detectable H3K4me3 peak. After 6 days of culture, as monocytes develop into macrophages, we observed a decrease in H3K27 acetylation in 1240 promoters and increase in 1307 promoters (z test, $P < 0.05$). Hence, at the epigenetic level, approximately equal numbers of promoters are turned on or off during macrophage differentiation (Fig. 1D). In general, H3K4me3 mark is largely constant at promoters that display dynamic H3K27 acetylation (Fig. 1D), suggesting that H3K27ac appears to function more as a mark of changes in promoter activity than H3K4me3.

In addition, as monocytes develop into macrophages, dynamic distal regulatory elements were operationally defined by H3K27ac at regions that are not known TSSs marked with H3K4me3 signal and that significantly (z test, $P < 0.05$) lose (2142) or gain (1894) acetylation (Fig. 1D). We observed that distal regulatory elements that gain H3K27ac generally gain H3K4me1, starting from a low level of H3K4me1. However, elements that lose H3K27ac generally do not lose their H3K4me1 mark, supporting the notion that H3K4me1 provides an epigenetic memory function in macrophages (Fig. 1, D and E) (*18*). Furthermore, DNase I cleavage frequencies reveal that the majority of distal regulatory DNA elements that lose H3K27ac remain accessible in macrophages (see also Fig. 2A).

To evaluate the relation between H3K27ac-bearing elements and gene expression, we plotted the relative change (fold change) in RNA level of the closest gene against H3K27ac distal elements, revealing a positive correlation between epigenomic marking and transcription from the closest dynamic gene (Fig. 1F). In contrast, the H3K4me1 mark does not correlate well with adjacent gene expression changes (Fig. 1G). This observation is in line with the hypothesis that H3K4me1 marks active (*23*, *24*) as well as latent regulatory elements (*18*). Altogether, our analysis indicates that in the course of monocyte-to-macrophage differentiation, histone H3 marks correlate positively with the activity of promoters (H3K4me3/H3K27ac) and distal regulatory elements that are presumed enhancers (H3K4me1/H3K27ac).

Biological pathways correlated with epigenetic marks

To identify the biological processes affected during differentiation of monocytes into macrophages, we performed a Gene Ontology (GO) analysis on differentially expressed genes (851 down, 1292 up) (table S1). We observed previously described differences in gene expression between monocytes and monocyte-derived macrophages, including the response to wounding (GO:0009611), inflammatory response (GO:0006954), and defense response (GO:0006952) (Fig. 1J and table S2) (*26*–*29*). As expected, pathogen-associated molecular patterns (PAMP)–mediated signal transduction through pattern recognition receptors (PRRs) is remodeled as monocytes differentiate into macrophages through changes in the epigenetic and transcription state of PRR genes. Furthermore, the nuclear factor κB (NF-κB) transcription factor (TF) subunits REL, RELA, RELB, NF-κB1, and NF-κB2, which are key regulators of the cellular response to inflammation (*30*), are all down-regulated (>2-fold lower) (Fig. 1H). Among the modulated inflammatory pathways during monocyte-to-macrophage differentiation, we detected components of the inflammasome (*31*) (Fig. 1H). In line with the expectation that tissue macrophages are more tolerant to challenges of the immune system, in vitro–differentiated macrophages, unlike monocytes, showed no activation of the inflammasome component caspase-1, and they lacked the capacity to secrete the active form of the proinflammatory IL-1β obtained after maturation of pro-IL-1β by caspase-1 (*32*) (Fig. 1I and fig. S4).

The most important GO terms associated with induced RNA expression during monocyte-to-macrophage differentiation (table S2) were monocarboxylic acid and cellular ketone metabolic processes. Up-regulated metabolic enzymes include dehydrogenases HSD17B1, -B4, and -B7—of which HSDB4 has been implicated in the peroxisomal beta-oxidation pathway and peroxisome proliferator–activated receptor (PPAR) signaling—which play essential roles in the regulation of cellular development and metabolism, as well as enzymes involved in glycine, serine, and threonine metabolism (*33*) and the tricarboxylic acid (TCA) cycle. The TCA cycle, which has recently been shown together with glycolysis to enhance endoplasmic reticulum (ER) and Golgi membrane synthesis and induce innate activation of dendritic cells upon Toll-like receptor (TLR)–mediated stimulation (*34*), appears to be remodeled such that the cytoplasmic versions of isocitrate dehydrogenase (IDH1) and malate dehydrogenase (MDH1) are induced >50 and >10-fold respectively, while their mitochondrial counterparts are induced about 2-fold, reaching ~20% of their cytoplasmic equivalents. These data support that re-orchestration of cellular metabolism during macrophage differentiation is an important component of the phenotypic switch between inflammatory and tolerant cells, with resting or tolerant macrophages exhibiting the TCA cycle and oxidative metabolism (*35*). The balance between glycolysis and oxidative metabolism also plays a role in trained immunity and tolerance [see the accompanying manuscript of Cheng *et al.* (*36*)].

The epigenetic profiles of tolerant versus trained cells

After an infectious episode, monocytes can retain an "immunological scar" from a previous encounter, entering either in a refractory state (tolerance) or a state of increased responsiveness (trained). These processes that result in nonspecific innate immune memory have been suggested to be mediated through epigenetic mechanisms (*10*, *19*) and describe very important in vivo phenomena such as postsepsis immunoparalysis (tolerance), or BCG-induced nonspecific (or heterologous) protective effects (training). Tolerance and training can be recapitulated in vitro using Mo exposed for 24 hours with LPS or β-glucan, respectively, followed by culture without additional stimuli for 5 days. These procedures yield differentiated cells that are either tolerant or trained macrophage-like cells (*10*) (Fig. 1A and fig. S4E).

At the epigenomic level, 17% of all dynamic promoters (ACp1) and 40.3% of all dynamic distal elements (ACe1) gain H3K27ac de novo exclusively in BG-Mf. Furthermore, a small subset of the dynamic distal regulatory elements (6%; ACe5) gain de novo H3K27ac marks exclusively in LPS-stimulated cells (LPS-Mf). These changes likely underlie the long-term effects of cell tolerization or training (Fig. 2, A and B, and table S3), mirroring postsepsis immunoparalysis and postvaccination nonspecific (heterologous) protection, respectively.

For the distal regulatory elements, consistent loss of H3K27ac is observed in Mf, LPS-Mf, and BG-Mf at 2142 distal elements (ACe2) (Fig. 2A) relative to the starting Mo. Distal elements that are marked de novo with H3K27ac, following differentiation from Mo to macrophages (Mf, LPS-Mf, and BG-Mf), fall into two clusters: ACe3, which shows a consistent gain of H3K27ac, and ACe4, which are dampened relative to macrophages concordantly in both LPS and β-glucan pretreated

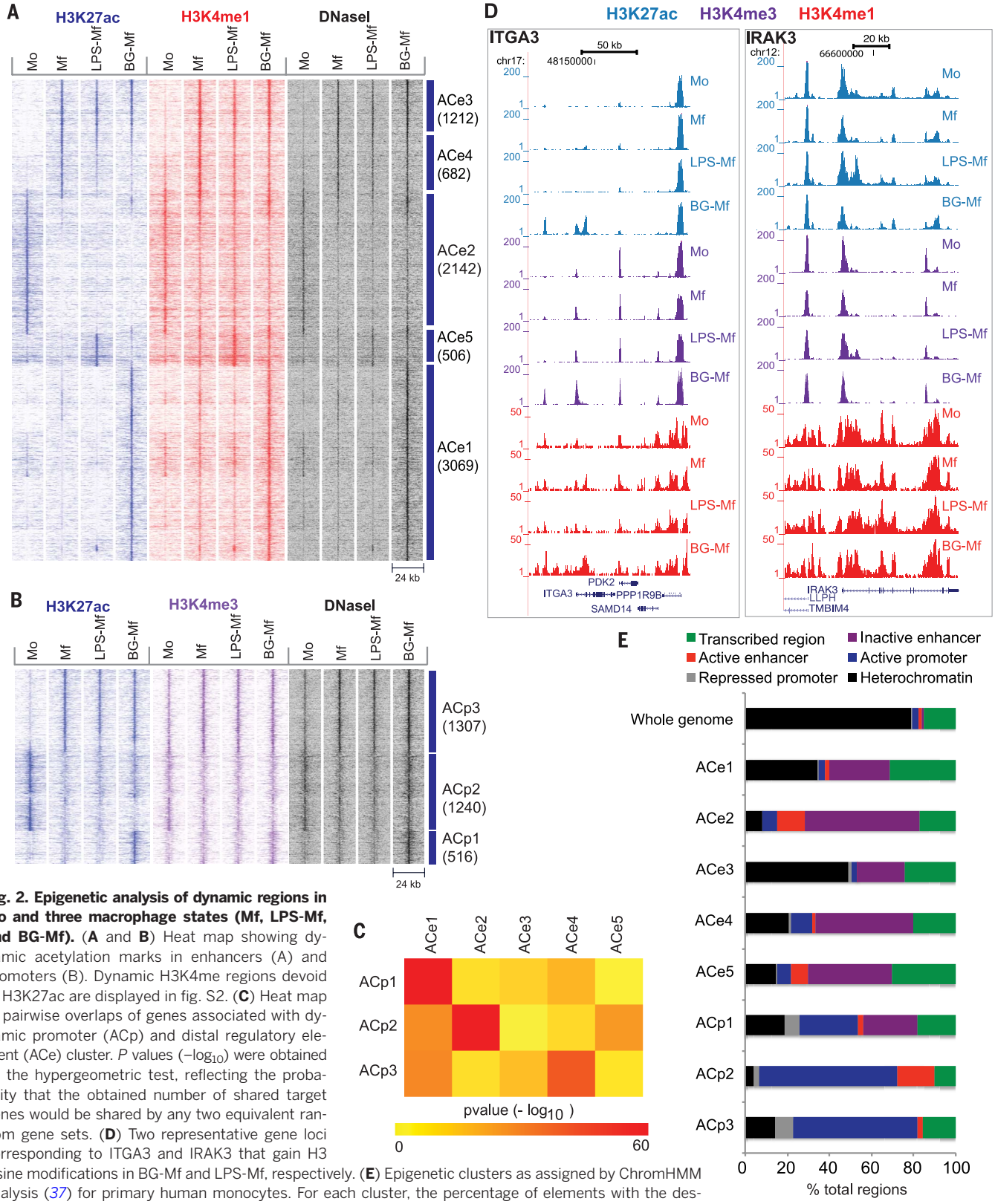

Fig. 2. Epigenetic analysis of dynamic regions in Mo and three macrophage states (Mf, LPS-Mf, and BG-Mf). (**A** and **B**) Heat map showing dynamic acetylation marks in enhancers (A) and promoters (B). Dynamic H3K4me regions devoid of H3K27ac are displayed in fig. S2. (**C**) Heat map of pairwise overlaps of genes associated with dynamic promoter (ACp) and distal regulatory element (ACe) cluster. *P* values ($-\log_{10}$) were obtained by the hypergeometric test, reflecting the probability that the obtained number of shared target genes would be shared by any two equivalent random gene sets. (**D**) Two representative gene loci corresponding to ITGA3 and IRAK3 that gain H3 lysine modifications in BG-Mf and LPS-Mf, respectively. (**E**) Epigenetic clusters as assigned by ChromHMM analysis (*37*) for primary human monocytes. For each cluster, the percentage of elements with the designations heterochromatic (H3K9me3, H3K27me3, or empty), active promoter (H3K4me3), inactive promoter (H3K4me3 and H3K27me3), active regulatory element (H3K4me1 and H3K27ac), inactive regulatory element (H3K4me1), and transcribed segment (H3K36me3) was calculated.

cells (Fig. 2A). The most extensive pretreatment-specific epigenetic response is obtained with β-glucan, whereby 3069 distal elements become marked by H3K27ac (ACe1) (Fig. 2, A and D, left panel). Some diversity in marking of distal elements with H3K27ac in ACe1 can be observed in other states: There are subclusters with low marking in Mf, or in Mo, and there is also a very small subcluster of ACe1 distal elements that is specifically marked upon LPS treatment (Fig. 2A). This indicates a modular, treatment-dependent activation of distinct pathways. Altogether, β-glucan appears to induce an epigenetic program that involves many promoters and distal elements. Some parts of this program are shared with untreated, naïve Mf and others with LPS-Mf, whereas neither LPS-tolerized nor naïve macrophages show such a strong exclusive epigenomic signature (Fig. 2, A and B).

We counted the genes targeted by more than one epigenetically marked cluster and computed the probability of randomly obtaining such overlaps (Fig. 2C). The most significant overlaps (hypergeometric test, $P < 0.01$) are between elements that show similar dynamics (ACp1/ACe1, ACp2/ACe2, and ACp3/ACe4), in keeping with the idea that epigenetically marked promoters and enhancers cooperate to drive gene expression. Notably, β-glucan–induced ACe1 distal elements also appear to be associated with ACp2 and ACp3 promoters more often than expected, suggesting modulation of differentiation-sensitive promoters by β-glucan–induced enhancers. Finally, the ACe5 distal elements, which are marked only upon LPS tolerization, are associated with ACp2 promoters, which are down-regulated upon monocyte differentiation to macrophages. This suggests that LPS-Mf stimulate the activity of a subset of monocyte-specific genes in macrophages via ACe5 elements (Fig. 2C).

To determine the provenance of these epigenetic elements in more detail, we used the ChromHMM data generated by BLUEPRINT for primary human monocytes. ChromHMM indexes chromatin into functional states such as active or repressed promoters, distal regulatory element (enhancer), and heterochromatic (repressed) chromatin (*37*). The majority of dynamic acetylated promoters and distal regulatory elements were already marked with low but appreciable levels of H3K4me3 (promoters) or with H3K4me1 at distal elements in Mo, indicating changes in activity rather than in chromatin state during differentiation to Mf, LPS-Mf, or BG-Mf (Fig. 2E).

Polytomous analysis of the transcriptome of Mf, LPS-Mf, and BG-Mf

To gain insight into the effects of LPS and β-glucan on nonspecific innate immune memory, we grouped genes according to a Bayesian methodology (MMSEQ and MMDIFF) (*38*, *39*) and applied a polytomous model selection approach that allows for classifying genes according to their expression pattern by considering multiple conditions simultaneously instead of generating multiple pairwise comparisons. This approach

A

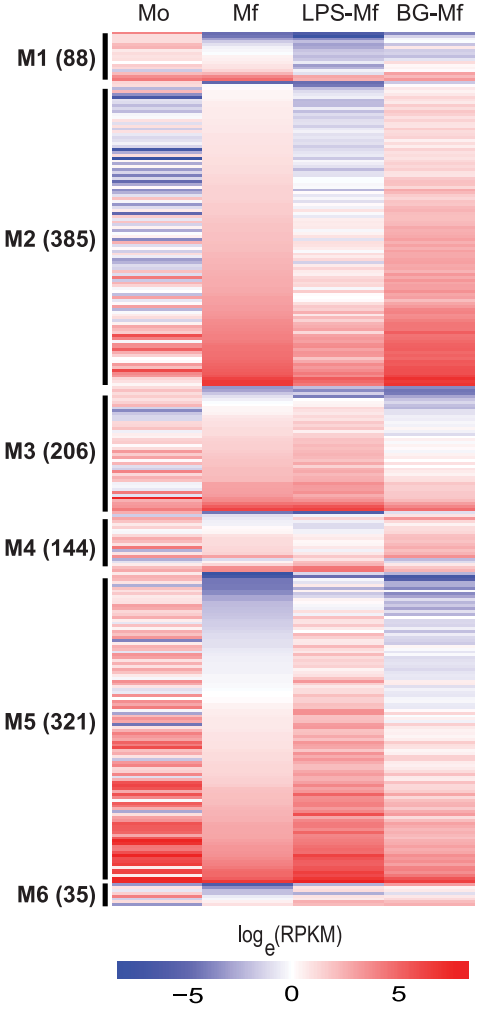

B

Module	GO term	Pvalue	Bonferroni
M1	sugar binding	1.70E-04	3.90E-02
M2	carboxylic acid metabolic process	4.00E-08	7.90E-05
	cellular ketone metabolic process	6.50E-08	1.30E-04
	oxidoreductase activity	2.10E-06	1.40E-03
	lipid metabolic process	5.40E-06	1.10E-02
M3	signal transducer activity	6.20E-06	2.40E-03
	receptor activity	5.60E-05	2.10E-02
M4	cofactor binding	1.00E-05	3.50E-03
M5	immune response	1.40E-22	3.00E-19
	response to wounding	2.30E-20	5.00E-17
	chemotaxis	2.40E-10	5.20E-07
	cytokine activity	1.70E-14	8.00E-12
	chemokine activity	7.80E-12	3.70E-09

C

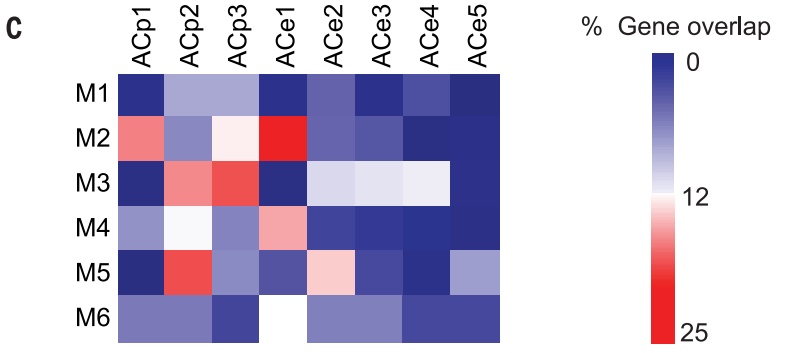

Fig. 3. GO analysis of epigenetic and transcript clusters in Mo and the three macrophage states (Mf, LPS-Mf, and BG-Mf). (**A**) Gene expression patterns were analyzed using a polytomous analysis of gene expression profiles that contrasts LPS-Mf and BG-Mf relative to Mf. Genes plotted are those with a fold change >4 and a polytomous post hoc probability >0.35. (**B**) Enriched GO categories in the major expression modules represented in Fig. 3A. (**C**) Heat map presentation of the percentage of genes in a module that overlap with a dynamic ACp or ACe cluster.

thus allowed us to identify statistically distinct expression patterns with biological relevance at once and define cell state–specific as well as co-regulated gene modules during monocyte-to-macrophage differentiation and in response to training or tolerization. A total of 14 models were compared to the base model of no differential expression and polytomous model selection was applied by computing the posterior probability of each model for each gene. Out of 11,698 genes that expressed >2 RPKM (reads per kilobase per million reads mapped), 7514 showed more than 2-fold changes, and 5847 fit one of the models with a posterior probability > 0.35. The models were condensed into expression modules (M1-6) to bring together genes as a function of their differential expression in LPS-Mf and BG-Mf relative to Mf cells. The genes of the modules that changed 4-fold are plotted in Fig. 3A, and the top associated GO terms are shown (Fig. 3B and tables S2 and S4). Interestingly, GO analysis on these modules (Fig. 3B) resulted in obtaining similar terms from our comparison of Mo and Mf in the absence of LPS or β-glucan (Figs. 1J and 3B). This suggests that both LPS and β-glucan pretreatments modulate the monocyte-to-macrophage differentiation program.

Modules are condition and cell specific

To link the expression modules to the epigenome, we determined the percentage of the genes of each module associated with an epigenetically dynamic promoter or distal element cluster (Fig. 3C and tables S3 and S4). Surprisingly, LPS-Mf do not down-regulate a large set of genes that are expressed in Mo to the same extent as Mf and BG-Mf (Fig. 3A, M5), suggesting that the LPS-Mf retains a monocyte-like expression level for these genes. Indeed, module M5 is enriched in genes from the GO categories "immune response," "response to wounding," and "chemotaxis" (Fig. 3B) and shows up-regulation of monocyte-specific genes (Fig. 1J), as well as a "response to LPS" (table S2). An example of a gene with a monocyte-like expression level in LPS-Mf is interleukin-1 receptor–associated kinase 3 (IRAK3), an essential regulator of innate immune homeostasis that functions as a negative-feedback regulator of Toll-like receptor signaling (*40*) (*41*) (Fig. 2D, right panel). This finding is expected from the perspective of the low inflammatory profile of tolerant macrophages. Module M5 harbors relatively many ACp2, ACe2, and ACe5 elements (Fig. 3C), suggesting that some parts of the monocyte-specific gene expression program are retained in LPS-Mf cells, possibly via induction of a new set of distal elements (ACe5). Furthermore, some of these elements may sustain the expression of target genes that are otherwise down-regulated in Mf and BG-Mf cells. Similarly, module M3 is generally better expressed in LPS-Mf than BG-Mf. M3 includes factors involved in signal transduction, such as IL10RA involved in controlling intestinal inflammation (*42*), the aryl hydrocarbon receptor repressor AHRR that has been shown to be essential for endotoxin tolerance (*43*), and the adenosine receptor ADORA3. Module M3 genes often harbor ACp2, ACp3, ACe2, ACe3, and ACe4 elements, and call the GO terms "signal transducer activity" and "receptor activity" (Fig. 3B), likely reflecting functional linkage between the execution of the naïve macrophage differentiation program and the LPS- and β-glucan–induced epigenetic programs.

Strikingly, module M2 represents a large set of genes that tend to be induced in Mf and are markedly less expressed in LPS-Mf, but equally or even better induced in BG-Mf (Fig. 3A, M2). M2 invokes the GO metabolic terms "cellular ketone metabolic process" and "carboxylic acid metabolic process" that are significant macrophage differentiation markers (Fig. 1J and table S2). Notably, M2 harbors ATF3, a transcription repressor known to target cytokine genes in mouse macrophages (*44*) (see also Fig. 4B). Module M4 is also most up-regulated in β-glucan pretreated cells, and, like M2, it is enriched in ACe1 distal elements (Fig. 3C). This suggests that sustained expression of module M4 in BG-Mf relative to the starting monocytes may depend on the presence of β-glucan–induced distal elements, explaining the apparently paradoxical overlap between the ACe1 elements and ACp2 promoters (Fig. 2C). M4 is enriched in the GO category "cofactor binding," including the pentose phosphate pathway–linked enzymes pyridoxine kinase PDXK and glucose-6-phosphate dehydrogenase G6PD, the glycolysis enzyme pyruvate dehydrogenase subunit DLAT, and the cytoplasmic version of the TCA cycle enzyme malate dehydrogenase MDH1 (table S2); also see (*36*). Intriguingly, a small subset of mitosis-specific genes that were previously reported in the context of monocyte-derived macrophages (*27*, *29*) are also present in module M4 (table S4). However, we assayed DNA replication directly and found no indication that Mf or BG-Mf cells are replicating (fig. S5).

Multiple modules contain G protein–coupled receptors (GPCRs), protein kinases, and epigenetic enzymes (fig. S6 and table S4), indicating extensive remodeling of the trained cell's repertoire of signal transduction molecules. Indeed, the β-adrenergic receptor ADRA2B is specifically induced in β-glucan–trained, rather than in LPS-tolerized, cells. Furthermore, monocytes and the three Mf states could be distinguished by differential expression of human adenosine receptor and Src kinase family members (*27*) (fig. S6). ADORA2B and the Fgr kinase are most strongly expressed in trained BG-Mf cells, whereas Hck kinase transcript levels are highest in LPS-Mf, providing potential pharmacological entry points to modulate immunoparalysis and trained innate immunity-related health conditions.

In summary, the epigenetic effects observed in BG-Mf and LPS-Mf appear to modulate the well-documented M-CSF–induced macrophage differentiation program (*26*), and polytomous transcriptome analysis reveals that LPS-Mf cells sustain expression of certain monocyte pro-inflammatory pathways that are dampened in Mf and BG-Mf cells (M3, M5). On the other hand, β-glucan pretreatment appears to reinforce specific gene expression programs, including metabolic pathway remodeling (M2, M4) through epigenetic modification of both ACp1 promoters and ACe1 distal regulatory elements.

The TF repertoires of differentiation, tolerance, and training

TFs bind to specific DNA sequences and are the effectors of cell phenotype and function, including numerous signal transduction pathways. As they recruit chromatin-modifying enzymes (fig. S6), which modulate gene expression, they are cornerstones of epigenetic signaling. Hence, we focused on the expression patterns of the human TFs to identify those whose expression patterns may determine Mo and the monocyte-derived macrophage fates (Mf, LPS-Mf, and BG-Mf). There are about 1600 bona fide human sequence–specific TFs (table S5). Of these, 74% are expressed at a detectable level (RPKM > 0.1), and 41% are expressed above 2 RPKM (Fig. 4A). Of the highly expressed TFs, 197 TFs change transcript levels more than 4-fold between at least two states (Mo, Mf, LPS-Mf, and BG-Mf) and are henceforth referred to as dynamic TFs. Altogether, 92 TFs are 4-fold down- and 105 TFs are 4-fold up-regulated (Fig. 4, B and C).

From a differentiation program perspective, it is informative to study dynamic changes within TF families (Fig. 4A). The largest TF superfamily is the C2H2 zinc finger Krueppel factors with and without Krueppel-associated box (KRAB) domains, encompassing 559 factors (Fig. 4A). Of these, 15% are dynamic, 14 are down-regulated, and 75 are up-regulated, albeit to low levels (Fig. 4, B and C).

Of the 48 human nuclear receptors, 26 are expressed in at least one of our four cell types, and eight are dynamic. Mo express relatively high levels (RPKM > 100) of the three proinflammatory NR4A1-3 nuclear receptor subfamily members NUR77, NURR1, and NOR1 (*45*), whereas derived macrophages show a dramatic reduction in expression of these nuclear receptors (Fig. 4B). The retinoic acid receptor RARA (NR1B1) also follows this pattern (Fig. 4B). On the other hand, LXRα (NR1H3), a nuclear receptor implicated among others in liver cell and macrophage cholesterol metabolism (*46*, *47*), increases in Mf, LPS-Mf, and BG-Mf cells (85-, 50- and 117-fold), attaining 300 RPKM in BG-Mf (Fig. 4C). Accordingly, the cytochrome (CYP27A1), an enzyme involved in the formation and breakdown of various molecules such as the 25-hydroxy-7-dehydrocholesterol that activates the LXRα (*48*), is itself induced ~25-fold in macrophages. Interestingly, the peroxisome proliferator-activated receptor PPARG (NR1C3) is reduced in Mf and LPS-Mf, but it is maintained in BG-Mf relative to purified Mo, in line with its proposed role in inflammation resolution (*49*) (Fig. 4B). Thus, nuclear receptors appear as major regulators of monocyte and macrophage biology, with LXRα levels qualitatively reflecting the immunological phenotypes of Mf, LPS-Mf, and BG-Mf (Fig. 1A).

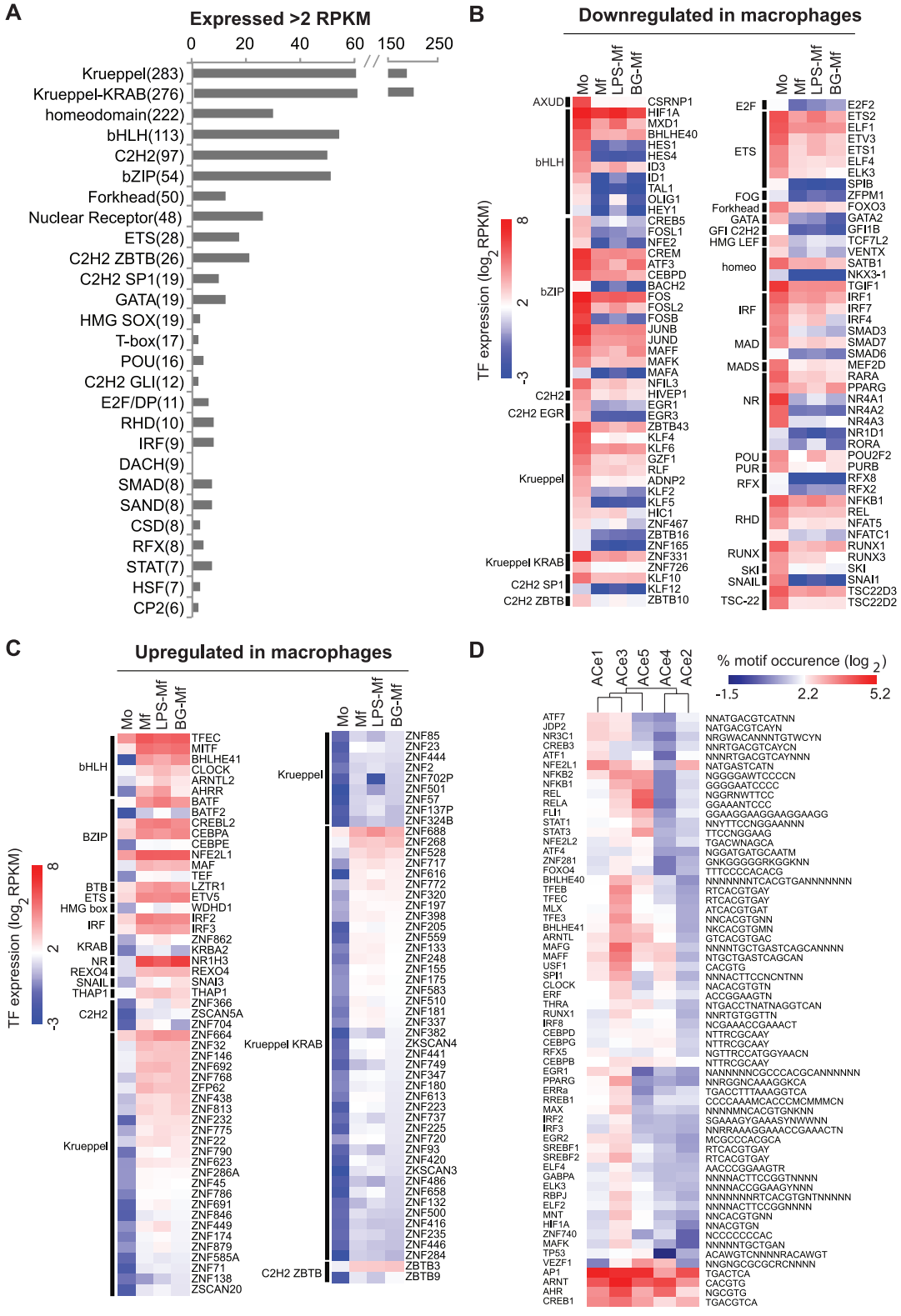

Fig. 4. The TF repertoires of monocytes and derived macrophages. (**A**) Bar representation of the TF family members that are expressed in at least one of the four cell samples (Mo, Mf, LPS-Mf, and BG-Mf). The number of TFs with RPKM values > 2 is plotted, and the total number of TF family members in humans is indicated between brackets. (**B** and **C**) Heat map of the expression levels (log_2 RPKM) of TFs that change expression at least 4-fold in at least one of the four conditions examined. TFs are grouped according to families and whether they are up- or down-regulated upon differentiation. Scale (left) indicates the level of expression (log_2 RPKM). (**D**) Hierarchical clustering of the TF motif occurrence frequency (log_2 percentage, scale at top) in each ACe cluster–associated DHS from all TF motifs that have more than 5% occurrence in at least one instance and that are overrepresented in at least one of the ACe clusters compared with all nondynamic acetylated regions (hypergeometric test, $P < 0.01$).

Aside from nuclear receptors, multiple TF families display coordinated family member switches. For instance, SNAI1, a major mesoderm lineage marker (*50*, *51*), is reduced in expression about 100-fold during macrophage differentiation, but its paralog SNAI3 is 5- to 10-fold higher in macrophages, most likely outcompeting SNAI1 for binding to its cognate DNA binding sites in Mfs (Fig. 4, B and C). Interferons (IFNs) and IFN responses are one essential arm of the host immune responses. Upon infection, PAMPs recognition by PRRs elicits antimicrobial responses by inducing target genes that include those encoding type I IFNs, proinflammatory cytokines, and chemokines. The interferon regulatory factor (IRF) family are transcriptional regulators of type I IFNs and IFN-inducible genes and help regulate facets of innate and adaptive immune responses (*52*). Five of the nine human IRFs are dynamic, as IRF1, IRF4, and IRF7 significantly decrease while IRF2 and IRF3 increase, in a background where IRF8 and IRF9 remain the most abundantly expressed IRF family members. This may reflect the decrease in IRF1 levels, which activates type I interferon IFN-β production, whereas levels of its antagonistic family member IRF2 increase (*53*–*55*). Thus, specific remodeling within TF families occurs in the course of monocyte-to-macrophage differentiation.

The basic leucine zipper domain (bZIP) TFs appear as an influential family in the course of monocyte differentiation, because 94% are expressed above 2 RPKM and 44% are dynamic (Fig. 4, A to C). AP1 complexes composed of heterodimers of the bZIP–FOS (FBJ murine osteosarcoma viral oncogene homolog) and -jun proto-oncogene (JUN) subfamilies are the most abundantly expressed (RPKM > 200) in monocytes and are reduced upon monocyte-to-macrophage differentiation (Fig. 4B), suggesting a down-modulation of AP1 signaling pathways. The CCAAT/enhancer-binding (C/EBP) bZIP subfamily also shows strong dynamics; CEBPA is induced 7-fold, whereas the paralog CEBPD is down-regulated 4-fold, indicating that there may be a coordinated switch in C/EBP heterodimerization which occurs in a complex along with the nondynamic, highly expressed CEBPB (Fig. 4, B and C). The 10-fold down-regulation of cAMP response element modulator (CREM), a bZIP subfamily member, also likely reflects a biological impact (Fig. 4B) because CREM codes for a dominant-negative heterodimerization partner of most cyclic adenosine monophosphate (cAMP) response element (CRE) binding proteins (*56*). CREM down-regulation is therefore likely to capacitate cAMP response element binding factors (see below).

Integration of epigenetic regions with TF binding sites

We used 1406 sequence motifs for 658 human TFs (*57*, *58*) to scan DNase I hypersensitive sites (DHSs) for TF-binding motifs. We determined the overlap between DHSs and dynamic distal elements in our data set. We performed hypergeometric tests using the motif frequency in all distal (nondynamic) H3K27ac regions as the background, to yield TF motifs that are likely candidates to regulate the activity of the distal regulatory regions. As an example, Fig. 4D plots the proportion of dynamically acetylated regions within one cluster that bear a given motif in their associated DHSs. To be included, a motif had to occur in at least 5% of any one epigenetically marked cluster (Fig. 4D and table S6). This reveals enriched TF motifs and permits a comparative analysis of putative TF repertoires in epigenetically marked regions.

The motifs for the bZIP AP1 and CREB1, and basic helix-loop-helix (bHLH) factors ARNT (aryl hydrocarbon receptor nuclear translocator) and AHR (aryl hydrocarbon receptor) are the most abundant occurring in 10 to 36% of ACe1- to ACe5-associated DHSs, in keeping with a broad role for the pathways that control these TFs in monocytes and macrophages, namely MAPKs (mitogen-activated protein kinases), cAMP, and metabolic signaling (*59*). Motifs for bZIP (sub-) family members, most prominently ATF1, ATF7, CREB3, and JDP2, are enriched in the β-glucan–induced ACe1 cluster. Furthermore, motif for the glucocorticoid receptor (NR3C1) is also relatively enriched in ACe1. This suggests that cAMP and cortisol-mediated signaling pathways intersect with the epigenetic response instigated by β-glucan training. By contrast, the immunoparalyzed LPS-Mf cell–specific ACe5 cluster is characterized by NF-κB and REL motifs (Fig. 4D), which are also present in the monocyte-specific ACe2 cluster (Fig. 1H). This is in keeping with the RNA-seq analysis, which points to a large transcriptome module (M5) where LPS-Mf cells resemble Mo more than naïve Mf or BG-Mf (Fig. 3A). In fact, module M5 harbors the NF-κB complex subunit genes that are known to be involved in inflammatory pathways.

Interestingly, the TF motif frequencies in the monocyte-specific ACe2 dynamic distal regions resemble those of ACe4 regions, which are induced in Mf but suppressed when monocytes are challenged with LPS or with β-glucan. However, ACe2 and ACe4 are distinguished by the enrichment of bZIP macrophage (MAFF and MAFG) (*60*, *61*) subfamily motifs in ACe4, which are also relatively more frequent in the differentiation-linked epigenetic clusters ACe1, ACe3, and ACe5, and thus likely drive ACe4 element activity upon differentiation.

The bHLH family, including the cAMP hypoxia inducible factor HIF1A, as well as the circadian factors BHLHE40, BHLHE41, and CLOCK (clock circadian regulator) (fig. S7) (*62*, *63*), show related patterns and are most frequent in the monocyte-to-macrophage differentiation cluster ACe3 and the least frequent in the monocyte-specific cluster ACe2. This suggests that bHLH TFs play important roles in macrophage differentiation. Moreover, IRF motifs are also enriched in the Mf differentiation cluster ACe3, as are smaller TF families such as EGR (early growth response) and ETS (E-twenty-six) factors (Fig. 4D).

In summary, the immune-tolerant phenotype elicited by LPS exposure appears to depend on epigenetically marked putative distal regulatory regions that frequently harbor NF-κB motifs, whereas the motifs that are enriched in the trained BG-Mf–marked epigenetic elements are most frequently also in epigenetic regions turned on in Mf, indicating reinforcement of specific Mf (sub-) programs by monocyte exposure to β-glucan.

Importance of cAMP-dependent intracellular signaling for trained immunity

cAMP signals start with a GPCR and culminate in cAMP-dependent protein kinase (PKA)–mediated CRE binding protein activation. cAMP-dependent signaling has been associated with monocyte function, differentiation, and response to infection (*64*, *65*). In Mf, BG-trained, and LPS-induced tolerant cells, the heterotrimeric G protein repertoire is remodeled: Adenylate cyclase 3 (ADCY3) and the cAMP-degrading phosphodiesterase (PDE3B) are specifically induced in trained cells (Fig. 5A and fig. S8). Strengthening the hypothesis that β-glucan training and LPS tolerization differ with respect to cAMP metabolism, we found that LPS-Mf express significantly more of the monocyte-specific cAMP phosphodiesterase (PDE4B) (Fig. 5A and fig. S8). The PKA regulatory subunit anchoring factor AKAP11 transcript is induced (two-tailed t test, $P < 0.05$) in Mf, BG-Mf, and LPS-Mf cells compared to Mo, and so is the type 1 alpha PKA regulatory subunit PRKAR1A. Furthermore, one of the five human PKA isoforms (PRKACB) is more highly induced (two-tailed t test, $P < 0.05$) in BG-Mf relative to LPS-Mf cells. In addition, the transcripts for CRE binding protein ATF3 and the ER stress response element binding CREB3L2 are higher in BG-Mf than in LPS-Mf (Fig. 5A and fig. S8). Importantly, we identified a known cAMP-inducible bHLH factor (*66*, *67*), BHLHE41, as a likely key TF motif enriched in ACe1, -3, -4, and -5 (Fig. 4D), strongly suggesting that cAMP-mediated molecular signal transduction is important for Mf, LPS-Mf, and BG-Mf cells.

We investigated the role of cAMP-dependent signaling in vitro and in an in vivo experimental model (Fig. 5B). Inhibition of adenylate cyclase and subsequent cAMP synthesis by 2′,5′-dideoxyadenosine significantly (Wilcoxon signed-rank test, $P < 0.05$) impairs training-induced increased cytokine production (Fig. 5C) and, in line with this, the PKA inhibitor H89 also blocks training of monocytes (Fig. 5D). Of note, the PKA inhibitor H89 had no effect on the LPS-triggered immune response (3% increased IL-6 production and 9% decreased TNFα production compared with control stimulation; $P > 0.05$) (fig. S9). Similar effects were observed with propranolol, an inhibitor of β-adrenergic signaling-dependent increase in cAMP (Fig. 5E). Importantly, even though the amplitude of responsiveness to secondary stimulation of each individual varies, the effect of the cAMP-pathway inhibitors on the trained immunity response is consistent and significant among the 18 tested individuals. A nonlethal infection with *C. albicans* protects mice against lethal candidiasis in a T/B cell–independent fashion, due to monocyte-dependent

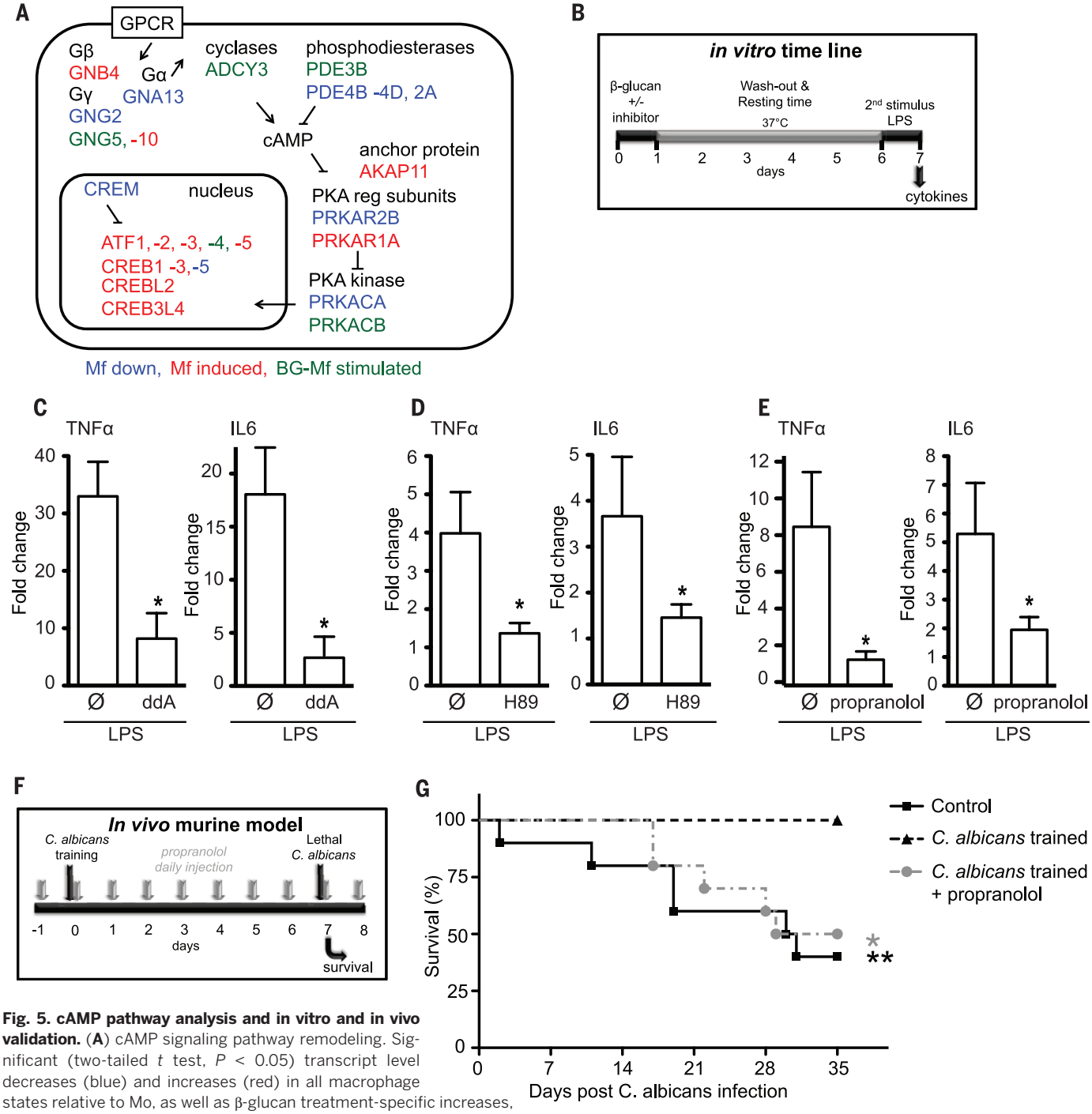

Fig. 5. cAMP pathway analysis and in vitro and in vivo validation. (**A**) cAMP signaling pathway remodeling. Significant (two-tailed *t* test, $P < 0.05$) transcript level decreases (blue) and increases (red) in all macrophage states relative to Mo, as well as β-glucan treatment-specific increases, are indicated; see also fig. S8. (**B**) Diagram of the timeline and experimental setup of the in vitro cAMP inhibition experiment. cAMP inhibitors or vehicle were applied to human primary monocytes during the first 24 hours of "training" [see fig. S4E and (*70*) for details]. After 6 days, secondary stimulation of cells was performed with LPS to induce cytokine production. (**C** to **E**) The inhibitor of adenylate cyclase 2′,5′-dideoxyadenosine (ddA), the PKA inhibitor H89, and the β-adrenergic receptor blocker propranolol inhibited the induction of training by β-glucan, assayed as the response to LPS stimulus on day 6. *$P < 0.05$ (Wilcoxon signed-rank test). Data show the fold increase in cytokine production (ELISA) upon training as compared with untrained Mf cells and are presented as mean ± SEM, $n > 6$ in three independent experiments. (**F**) Timeline of the in vivo training experiment in mice. Mice were either injected intravenously with phosphate-buffered saline (control) or a nonlethal dose of *C. albicans* [2×10^4 colony-forming units (CFU) per mouse] 7 days before intravenous inoculation of a lethal *C. albicans* dose (2×10^6 CFU per mouse). In a third group of mice, propranolol was administered before the inoculation of the nonlethal dose of *C. albicans* (*70*). (**G**) Survival rate of wild-type C57BL/6 mice to a systemic infection with *C. albicans* ($n \geq 8$ per group). Statistical significance between the groups (Kaplan and Meier) was calculated using the log-rank test. *$P < 0.05$, **$P < 0.01$ versus control animals.

trained immunity (*10*). The protection conferred by the nonlethal dose of *C. albicans* was completely abolished by the use of propranolol (Fig. 5, F and G), validating that cAMP-dependent signaling is important for the protective effects of trained immunity.

Discussion

Monocytes and macrophages are prototype mononuclear phagocytes that mediate fundamental innate immune processes such as pathogen clearance, inflammatory cytokine production, and tissue repair. We studied macrophages differentiated from monocytes exclusively in the presence of human serum. This is probably the in vitro model closest to the development of tissue-resident macrophages in vivo, because the differentiation is taking place under the influence of endogenous homeostatic levels of macrophage colony-stimulating factor (M-CSF), rather than stimulated by artificially high concentrations of recombinant CSFs (*68*). In contrast, differentiation with additional recombinant growth factors such as granulocyte macrophage (GM)-CSF, IL-4, or IFN-γ will induce activated M1 or M2 macrophages most often encountered during infectious processes (*68*). Thus, these observations provide clues as to which pathways to tackle in a clinical attempt to reverse immune tolerance to turn on training and activation pathways during immunoparalysis and sepsis.

The present work shows that differentiating monocytes undergo substantial epigenetic changes affecting ~19 mega base pairs (Mbp), equivalent to 0.6%, of the human genome. Using the guidelines of the International Human Epigenome Consortium, we generated genome-wide maps of histone modifications (H3K4me3, H3K4me1, H3K27ac, and DNase I accessibility). We delineated eight epigenetically marked clusters reflecting putative transcription regulatory regions, of which four are differentially modulated when monocytes are exposed to LPS or β-glucan. H3K27 acetylation levels changed at thousands of promoters and distal regions and correlate well with observed changes in gene expression.

Although we cannot ascertain what fraction of the purified monocytes that we cultured participated in any one observed epigenomic or transcriptome change, nor to what extent the laboratory in vitro conditions affect differentiating monocytes relative to the in vivo condition, we can state that monocytes are able to deploy a long-term epigenetic program upon β-glucan–induced training in vitro in the absence of DNA replication. This epigenetic program persists for at least 5 days, is highly reproducible across monocytes from unrelated donors, and represents β-glucan–induced changes in the epigenetic states of promoter and distal elements, indicative of a specific cell differentiation program. Although more modest, a similar epigenomic response of monocytes to LPS is also uncovered, which induces a state akin to post-sepsis immune paralysis. Identification of core signatures of training and tolerance is thus important, as it allows the better characterization of these functional states. Because many epigenetic clusters that differentiate training and tolerance yield significant GO scores, the clusters that we identified appear to report physiologically relevant effects. Indeed, we linked cAMP signaling to the trained phenotype in purified human monocytes, as well as in a mouse model of disseminated candidiasis.

Our TF analysis suggests that monocyte differentiation relies on quantitative remodeling of the TF repertoire, because coordinated changes affect multiple members of many TF families. DNA sequence motifs detected in DHSs adjacent to epigenetically dynamic elements link to cell state–specific epigenetic clusters that fit RNA expression modules. The present data sets, in particular the genomic coordinates of the dynamic epigenomic sites, therefore represent a rich molecular resource to understand and modulate the functionality of monocyte-derived medically important cell types such as macrophages, dendritic cells, foam cells, and osteoclasts (*69*).

Methodology

Monocyte and monocyte-derived cells

To enable analysis of the different functional programs of monocytes, human primary monocytes were purified from three to six healthy human donors (depending on experiment) by first isolating peripheral blood mononuclear cells by differential centrifugation over Ficoll-Paque, followed by depletion of T cells, B cells, and NK cells with beads coated with antibodies directed against CD3, CD19, and CD56, respectively (fig. S1). Mf were obtained by in vitro culture of the purified Mo for 6 days in cell culture medium enriched with human serum (10%). Monocyte tolerance, a state akin to immune paralysis during bacterial sepsis or endotoxin shock, was induced in vitro by exposing the purified monocytes to LPS for 24 hours (*9*). Monocyte training—a functional state in which cells respond more strongly to microbial stimuli that mirror the non-specific protective effects of live microorganism vaccination [e.g., BCG, measles, and yellow fever (*15*)] (Fig. 1, A and B)—was induced in vitro by exposing the purified monocytes to β-glucan for 24 hours (Fig. 1B) (*10*). The LPS or β-glucan was then washed out from the system, and the cells were incubated in enriched cell-cultured medium for 5 days.

Genome-wide epigenetic profiling

For all the four types of cells described above—Mo, Mf, LPS-Mf, and BG-Mf cells—the epigenomic profiles were generated for three histone H3-borne marks known to be associated with gene expression. They respectively mark promoters (H3K4me3), distal regulatory elements (H3K4me1), and the active forms of both promoters and enhancers (H3K27ac) (*23*, *24*). Additionally, RNA and DNase I accessibility were quantified (*25*). The raw data from the sequencing experiments are available through the European Genome-Phenome Archive (EGA), using the data set identifier EGAD00001001011. Please apply to the Blueprint Data Access Committee (http://www.blueprint-epigenome.eu/index.cfm?p=B5E93EE0-09E2-5736-A708817C27EF2DB7) for permission to access this data set. Processed data can be accessed via Gene Expression Omnibus (GEO) accession no. GSE58310.

REFERENCES AND NOTES

1. J. S. Lewis, J. A. Lee, J. C. Underwood, A. L. Harris, C. E. Lewis, Macrophage responses to hypoxia: Relevance to disease mechanisms. *J. Leukoc. Biol.* **66**, 889–900 (1999). pmid: 10614769
2. F. Geissmann *et al*., Development of monocytes, macrophages, and dendritic cells. *Science* **327**, 656–661 (2010). doi: 10.1126/science.1178331; pmid: 20133564
3. C. Auffray, M. H. Sieweke, F. Geissmann, Blood monocytes: Development, heterogeneity, and relationship with dendritic cells. *Annu. Rev. Immunol.* **27**, 669–692 (2009). doi: 10.1146/annurev.immunol.021908.132557; pmid: 19132917
4. L. C. Davies, S. J. Jenkins, J. E. Allen, P. R. Taylor, Tissue-resident macrophages. *Nat. Immunol.* **14**, 986–995 (2013). doi: 10.1038/ni.2705; pmid: 24048120
5. F. Ginhoux, S. Jung, Monocytes and macrophages: Developmental pathways and tissue homeostasis. *Nat. Rev. Immunol.* **14**, 392–404 (2014). doi: 10.1038/nri3671; pmid: 24854589
6. C. Jakubzick *et al*., Minimal differentiation of classical monocytes as they survey steady-state tissues and transport antigen to lymph nodes. *Immunity* **39**, 599–610 (2013). doi: 10.1016/j.immuni.2013.08.007; pmid: 24012416
7. E. Zigmond *et al*., Ly6C hi monocytes in the inflamed colon give rise to proinflammatory effector cells and migratory antigen-presenting cells. *Immunity* **37**, 1076–1090 (2012). doi: 10.1016/j.immuni.2012.08.026; pmid: 23219392
8. A. Sica, A. Mantovani, Macrophage plasticity and polarization: In vivo veritas. *J. Clin. Invest.* **122**, 787–795 (2012). doi: 10.1172/JCI59643; pmid: 22378047
9. S. K. Biswas, E. Lopez-Collazo, Endotoxin tolerance: New mechanisms, molecules and clinical significance. *Trends Immunol.* **30**, 475–487 (2009). doi: 10.1016/j.it.2009.07.009; pmid: 19781994
10. J. Quintin *et al*., *Candida albicans* infection affords protection against reinfection via functional reprogramming of monocytes. *Cell Host Microbe* **12**, 223–232 (2012). doi: 10.1016/j.chom.2012.06.006; pmid: 22901542
11. M. G. Netea, J. Quintin, J. W. van der Meer, Trained immunity: A memory for innate host defense. *Cell Host Microbe* **9**, 355–361 (2011). doi: 10.1016/j.chom.2011.04.006; pmid: 21575907
12. J. Quintin, S. C. Cheng, J. W. van der Meer, M. G. Netea, Innate immune memory: Towards a better understanding of host defense mechanisms. *Curr. Opin. Immunol.* **29**, 1–7 (2014). doi: 10.1016/j.coi.2014.02.006; pmid: 24637148
13. D. C. Ifrim *et al*., Trained immunity or tolerance: Opposing functional programs induced in human monocytes after engagement of various pattern recognition receptors. *Clin. Vaccine Immunol.* **21**, 534–545 (2014). doi: 10.1128/CVI.00688-13; pmid: 24521784
14. J. Kleinnijenhuis *et al*., Bacille Calmette-Guerin induces NOD2-dependent nonspecific protection from reinfection via epigenetic reprogramming of monocytes. *Proc. Natl. Acad. Sci. U.S.A.* **109**, 17537–17542 (2012). doi: 10.1073/pnas.1202870109; pmid: 22988082
15. C. S. Benn, M. G. Netea, L. K. Selin, P. Aaby, A small jab—a big effect: Nonspecific immunomodulation by vaccines. *Trends Immunol.* **34**, 431–439 (2013). doi: 10.1016/j.it.2013.04.004; pmid: 23680130
16. O. Takeuch, S. Akira, Epigenetic control of macrophage polarization. *Eur. J. Immunol.* **41**, 2490–2493 (2011). doi: 10.1002/eji.201141792; pmid: 21952803
17. M. Ishii *et al*., Epigenetic regulation of the alternatively activated macrophage phenotype. *Blood* **114**, 3244–3254 (2009). doi: 10.1182/blood-2009-04-217620; pmid: 19567879
18. R. Ostuni *et al*., Latent enhancers activated by stimulation in differentiated cells. *Cell* **152**, 157–171 (2013). doi: 10.1016/j.cell.2012.12.018; pmid: 23332752
19. S. L. Foster, D. C. Hargreaves, R. Medzhitov, Gene-specific control of inflammation by TLR-induced chromatin modifications. *Nature* **447**, 972–978 (2007). pmid: 17538624
20. D. Adams *et al*., BLUEPRINT to decode the epigenetic signature written in blood. *Nat. Biotechnol.* **30**, 224–226 (2012). doi: 10.1038/nbt.2153; pmid: 22398613

21. J. H. Martens, H. G. Stunnenberg, BLUEPRINT: Mapping human blood cell epigenomes. *Haematologica* **98**, 1487–1489 (2013). doi: 10.3324/haematol.2013.094243; pmid: 24091925
22. M. G. Netea *et al*., Differential requirement for the activation of the inflammasome for processing and release of IL-1beta in monocytes and macrophages. *Blood* **113**, 2324–2335 (2009). doi: 10.1182/blood-2008-03-146720; pmid: 19104081
23. N. D. Heintzman *et al*., Histone modifications at human enhancers reflect global cell-type-specific gene expression. *Nature* **459**, 108–112 (2009). doi: 10.1038/nature07829; pmid: 19295514
24. A. Rada-Iglesias *et al*., A unique chromatin signature uncovers early developmental enhancers in humans. *Nature* **470**, 279–283 (2011). doi: 10.1038/nature09692; pmid: 21160473
25. R. E. Thurman *et al*., The accessible chromatin landscape of the human genome. *Nature* **489**, 75–82 (2012). doi: 10.1038/nature11232; pmid: 22955617
26. S. Hashimoto, T. Suzuki, H. Y. Dong, N. Yamazaki, K. Matsushima, Serial analysis of gene expression in human monocytes and macrophages. *Blood* **94**, 837–844 (1999). pmid: 10419873
27. F. O. Martinez, S. Gordon, M. Locati, A. Mantovani, Transcriptional profiling of the human monocyte-to-macrophage differentiation and polarization: New molecules and patterns of gene expression. *J. Immunol.* **177**, 7303–7311 (2006). doi: 10.4049/jimmunol.177.10.7303; pmid: 17082649
28. J. Li *et al*., cDNA microarray analysis reveals fundamental differences in the expression profiles of primary human monocytes, monocyte-derived macrophages, and alveolar macrophages. *J. Leukoc. Biol.* **81**, 328–335 (2007). doi: 10.1189/jlb.0206124; pmid: 17046970
29. C. Dong *et al*., RNA sequencing and transcriptomal analysis of human monocyte to macrophage differentiation. *Gene* **519**, 279–287 (2013). doi: 10.1016/j.gene.2013.02.015; pmid: 23458880
30. S. Vallabhapurapu, M. Karin, Regulation and function of NF-kappaB transcription factors in the immune system. *Annu. Rev. Immunol.* **27**, 693–733 (2009). doi: 10.1146/annurev.immunol.021908.132641; pmid: 19302050
31. F. Martinon, J. Tschopp, Inflammatory caspases: Linking an intracellular innate immune system to autoinflammatory diseases. *Cell* **117**, 561–574 (2004). doi: 10.1016/j.cell.2004.05.004; pmid: 15163405
32. J. M. Bruey *et al*., PAN1/NALP2/PYPAF2, an inducible inflammatory mediator that regulates NF-kappaB and caspase-1 activation in macrophages. *J. Biol. Chem.* **279**, 51897–51907 (2004). doi: 10.1074/jbc.M406741200; pmid: 15456791
33. M. Jain *et al*., Metabolite profiling identifies a key role for glycine in rapid cancer cell proliferation. *Science* **336**, 1040–1044 (2012). doi: 10.1126/science.1218595; pmid: 22628656
34. B. Everts *et al*., TLR-driven early glycolytic reprogramming via the kinases TBK1-IKKε supports the anabolic demands of dendritic cell activation. *Nat. Immunol.* **15**, 323–332 (2014). doi: 10.1038/ni.2833; pmid: 24562310
35. S. K. Biswas, A. Mantovani, Orchestration of metabolism by macrophages. *Cell Metab.* **15**, 432–437 (2012). doi: 10.1016/j.cmet.2011.11.013; pmid: 22482726
36. S.-C. Cheng *et al*., mTOR/HIF1α-mediated aerobic glycolysis as metabolic basis for trained immunity. *Science* **345**, 1250684 (2014).
37. J. Ernst, M. Kellis, Discovery and characterization of chromatin states for systematic annotation of the human genome. *Nat. Biotechnol.* **28**, 817–825 (2010). doi: 10.1038/nbt.1662; pmid: 20657582
38. E. Turro *et al*., Haplotype and isoform specific expression estimation using multi-mapping RNA-seq reads. *Genome Biol.* **12**, R13 (2011). doi: 10.1186/gb-2011-12-2-r13; pmid: 21310039
39. E. Turro, W. J. Astle, S. Tavaré, Flexible analysis of RNA-seq data using mixed effects models. *Bioinformatics* **30**, 180–188 (2014). doi: 10.1093/bioinformatics/btt624; pmid: 24281695
40. K. Kobayashi *et al*., IRAK-M is a negative regulator of Toll-like receptor signaling. *Cell* **110**, 191–202 (2002). doi: 10.1016/S0092-8674(02)00827-9; pmid: 12150927
41. L. Balaci *et al*., IRAK-M is involved in the pathogenesis of early-onset persistent asthma. *Am. J. Hum. Genet.* **80**, 1103–1114 (2007). doi: 10.1086/518259; pmid: 17503328
42. D. S. Shouval *et al*., Interleukin 10 receptor signaling: Master regulator of intestinal mucosal homeostasis in mice and humans. *Adv. Immunol.* **122**, 177–210 (2014). doi: 10.1016/B978-0-12-800267-4.00005-5; pmid: 24507158
43. A. Bessede *et al*., Aryl hydrocarbon receptor control of a disease tolerance defence pathway. *Nature* **511**, 184–190 (2014). doi: 10.1038/nature13323; pmid: 24930766
44. C. H. Khuu, R. M. Barrozo, T. Hai, S. L. Weinstein, Activating transcription factor 3 (ATF3) represses the expression of CCL4 in murine macrophages. *Mol. Immunol.* **44**, 1598–1605 (2007). doi: 10.1016/j.molimm.2006.08.006; pmid: 16982098
45. J. P. McMorrow, E. P. Murphy, Inflammation: A role for NR4A orphan nuclear receptors? *Biochem. Soc. Trans.* **39**, 688–693 (2011). doi: 10.1042/BST0390688; pmid: 21428963
46. T. Kohro *et al*., Genomic structure and mapping of human orphan receptor LXR alpha: Upregulation of LXRa mRNA during monocyte to macrophage differentiation. *J. Atheroscler. Thromb.* **7**, 145–151 (2000). doi: 10.5551/jat1994.7.145; pmid: 11480455
47. M. Boergesen *et al*., Genome-wide profiling of liver X receptor, retinoid X receptor, and peroxisome proliferator-activated receptor α in mouse liver reveals extensive sharing of binding sites. *Mol. Cell. Biol.* **32**, 852–867 (2012). doi: 10.1128/MCB.06175-11; pmid: 22158963
48. K. Endo-Umeda *et al*., 7-Dehydrocholesterol metabolites produced by sterol 27-hydroxylase (CYP27A1) modulate liver X receptor activity. *J. Steroid Biochem. Mol. Biol.* **140**, 7–16 (2014). doi: 10.1016/j.jsbmb.2013.11.010; pmid: 24269243
49. E. L. Gautier *et al*., Systemic analysis of PPARγ in mouse macrophage populations reveals marked diversity in expression with critical roles in resolution of inflammation and airway immunity. *J. Immunol.* **189**, 2614–2624 (2012). doi: 10.4049/jimmunol.1200495; pmid: 22855714
50. B. Hotz, A. Visekruna, H. J. Buhr, H. G. Hotz, Beyond epithelial to mesenchymal transition: A novel role for the transcription factor Snail in inflammation and wound healing. *J. Gastrointest. Surg.* **14**, 388–397 (2010). doi: 10.1007/s11605-009-1068-3; pmid: 19856033
51. M. Leptin, twist and snail as positive and negative regulators during Drosophila mesoderm development. *Genes Dev.* **5**, 1568–1576 (1991). doi: 10.1101/gad.5.9.1568; pmid: 1884999
52. K. Ozato, P. Tailor, T. Kubota, The interferon regulatory factor family in host defense: Mechanism of action. *J. Biol. Chem.* **282**, 20065–20069 (2007). doi: 10.1074/jbc.R700003200; pmid: 17502370
53. M. Miyamoto *et al*., Regulated expression of a gene encoding a nuclear factor, IRF-1, that specifically binds to IFN-beta gene regulatory elements. *Cell* **54**, 903–913 (1988). doi: 10.1016/S0092-8674(88)91307-4; pmid: 3409321
54. H. Harada *et al*., Structurally similar but functionally distinct factors, IRF-1 and IRF-2, bind to the same regulatory elements of IFN and IFN-inducible genes. *Cell* **58**, 729–739 (1989). doi: 10.1016/0092-8674(89)90107-4; pmid: 2475256
55. R. Günthner, H. J. Anders, Interferon-regulatory factors determine macrophage phenotype polarization. *Mediators Inflamm.* **2013**, 731023 (2013). doi: 10.1155/2013/731023; pmid: 24379524
56. G. Servillo, M. A. Della Fazia, P. Sassone-Corsi, Coupling cAMP signaling to transcription in the liver: Pivotal role of CREB and CREM. *Exp. Cell Res.* **275**, 143–154 (2002). doi: 10.1006/excr.2002.5491; pmid: 11969286
57. A. Jolma *et al*., DNA-binding specificities of human transcription factors. *Cell* **152**, 327–339 (2013). doi: 10.1016/j.cell.2012.12.009; pmid: 23332764
58. S. J. van Heeringen, G. J. Veenstra, GimmeMotifs: A de novo motif prediction pipeline for ChIP-sequencing experiments. *Bioinformatics* **27**, 270–271 (2011). doi: 10.1093/bioinformatics/btq636; pmid: 21081511
59. K. Newton, V. M. Dixit, Signaling in innate immunity and inflammation. *Cold Spring Harb. Perspect. Biol.* **4**, a006049 (2012). doi: 10.1101/cshperspect.a006049; pmid: 22296764
60. T. Lange, S. Dimitrov, J. Born, Effects of sleep and circadian rhythm on the human immune system. *Ann. N.Y. Acad. Sci.* **1193**, 48–59 (2010). doi: 10.1111/j.1749-6632.2009.05300.x; pmid: 20398008
61. M. H. Sieweke, J. E. Allen, Beyond stem cells: Self-renewal of differentiated macrophages. *Science* **342**, 1242974 (2013). doi: 10.1126/science.1242974; pmid: 24264994
62. A. Aziz, E. Soucie, S. Sarrazin, M. H. Sieweke, MafB/c-Maf deficiency enables self-renewal of differentiated functional macrophages. *Science* **326**, 867–871 (2009). doi: 10.1126/science.1176056; pmid: 19892988
63. K. R. Stenmark *et al*., The adventitia: Essential regulator of vascular wall structure and function. *Annu. Rev. Physiol.* **75**, 23–47 (2013). doi: 10.1146/annurev-physiol-030212-183802; pmid: 23216413
64. G. D. Wenger, M. S. O'Dorisio, Induction of cAMP-dependent protein kinase I during human monocyte differentiation. *J. Immunol.* **134**, 1836–1843 (1985). pmid: 2981923
65. K. C. Bagley, S. F. Abdelwahab, R. G. Tuskan, T. R. Fouts, G. K. Lewis, Cholera toxin and heat-labile enterotoxin activate human monocyte-derived dendritic cells and dominantly inhibit cytokine production through a cyclic AMP-dependent pathway. *Infect. Immun.* **70**, 5533–5539 (2002). doi: 10.1128/IAI.70.10.5533-5539.2002; pmid: 12228279
66. M. Shen *et al*., Induction of basic helix-loop-helix protein DEC1 (BHLHB2)/Stra13/Sharp2 in response to the cyclic adenosine monophosphate pathway. *Eur. J. Cell Biol.* **80**, 329–334 (2001). doi: 10.1078/0171-9335-00167; pmid: 11432722
67. M. Shen *et al*., Molecular characterization of the novel basic helix-loop-helix protein DEC1 expressed in differentiated human embryo chondrocytes. *Biochem. Biophys. Res. Commun.* **236**, 294–298 (1997). doi: 10.1006/bbrc.1997.6960; pmid: 9240428
68. T. A. Wynn, A. Chawla, J. W. Pollard, Macrophage biology in development, homeostasis and disease. *Nature* **496**, 445–455 (2013). doi: 10.1038/nature12034; pmid: 23619691
69. S. Gordon, P. R. Taylor, Monocyte and macrophage heterogeneity. *Nat. Rev. Immunol.* **5**, 953–964 (2005). doi: 10.1038/nri1733; pmid: 16322748
70. Materials and methods are available as supplementary materials on *Science* Online.

ACKNOWLEDGMENTS

The authors are grateful to J. Stamatoyannopoulos for help with DNaseI-seq. We thank S. van Heeringen for access to his databases and expertise. The research leading to the results described in this manuscript has received funding from the European Union's Seventh Framework Programme (FP7/2007-2013) under grant agreement no. 282510-BLUEPRINT. M.G.N. was supported by a Vici grant of the Netherlands Organization for Scientific Research and an ERC Consolidator Grant (no. 310372) and J.H.A.M by a VIDI grant of the Netherlands Organization for Scientific Research. All the genome-wide data generated and analyzed in this study, as well as the sequencing details, can be accessed via GEO accession no. GSE58310.

SUPPLEMENTARY MATERIALS

www.sciencemag.org/content/345/6204/1251086/suppl/DC1
Materials and Methods
Figs. S1 to S9
Tables S1 to S6
References

20 January 2014; accepted 28 August 2014
10.1126/science.1251086

Science

Epigenetic programming of monocyte-to-macrophage differentiation and trained innate immunity

Sadia Saeed, Jessica Quintin, Hindrik H. D. Kerstens, Nagesha A. Rao, Ali Aghajanirefah, Filomena Matarese, Shih-Chin Cheng, Jacqueline Ratter, Kim Berentsen, Martijn A. van der Ent, Nilofar Sharifi, Eva M. Janssen-Megens, Menno Ter Huurne, Amit Mandoli, Tom van Schaik, Aylwin Ng, Frances Burden, Kate Downes, Mattia Frontini, Vinod Kumar, Evangelos J. Giamarellos-Bourboulis, Willem H. Ouwehand, Jos W. M. van der Meer, Leo A. B. Joosten, Cisca Wijmenga, Joost H. A. Martens, Ramnik J. Xavier, Colin Logie, Mihai G. Netea and Hendrik G. Stunnenberg

Science **345** (6204), 1251086.
DOI: 10.1126/science.1251086

A BLUEPRINT of immune cell development

To determine the epigenetic mechanisms that direct blood cells to develop into the many components of our immune system, the BLUEPRINT consortium examined the regulation of DNA and RNA transcription to dissect the molecular traits that govern blood cell differentiation. By inducing immune responses, Saeed *et al.* document the epigenetic changes in the genome that underlie immune cell differentiation. Cheng *et al.* demonstrate that trained monocytes are highly dependent on the breakdown of sugars in the presence of oxygen, which allows cells to produce the energy needed to mount an immune response. Chen *et al.* examine RNA transcripts and find that specific cell lineages use RNA transcripts of different length and composition (isoforms) to form proteins. Together, the studies reveal how epigenetic effects can drive the development of blood cells involved in the immune system.

Science, this issue 10.1126/science.1251086, 10.1126/science.1250684, 10.1126/science.1251033